Obrabotka metallov (tekhnologiya, oborudovanie, instrumenty) = Metal Working and Material Science. 2022 vol. 24 no. 4 pp. 206–218
ISSN: 1994-6309 (print) / 2541-819X (online)
DOI: 10.17212/1994-6309-2022-24.4-206-218

NSTU NETI

Obrabotka metallov - Metal Working and Material Science

Journal homepage: http://journals.nstu.ru/obrabotka_metallov

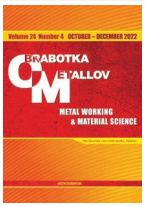

Effect of deformation processing on microstructure and mechanical properties of Ti-42Nb-7Zr alloy

Anna Eroshenko [1, a,*], *Elena Legostaeva* [1, b], *Ivan Glukhov* [1, c], *Pavel Uvarkin* [1, d], *Alexey Tolmachev* [1, e], *Nikita Luginin* [1, 2, f], *Vladimir Bataev* [3, g], *Ivan Ivanov* [3, h], *Yurii Sharkeev* [1, 2, i]

[1] Institute of Strength Physics and Materials Science of Siberian Branch Russian Academy of Sciences, 2/4 Akademicheskiy Av., 634055, Tomsk, Russia Federation
[2] Tomsk polytechnic university, 30 Lenin Av., 634050, Tomsk, Russia Federation
[3] Novosibirsk State Technical University, 20 Prospekt K. Marksa, Novosibirsk, 630073, Russian Federation

[a] https://orcid.org/0000-0001-8812-9287, eroshenko@ispms.ru, [b] https://orcid.org/0000-0003-3684-9930, lego@ispms.ru,
[c] https://orcid.org/0000-0001-5557-5950, gia@ispms.ru, [d] https://orcid.org/0000-0003-1169-3765, uvarkin@ispms.ru,
[e] https://orcid.org/0000-0003-4669-8478, tolmach@ispms.ru, [f] https://orcid.org/0000-0001-6504-8193, nikishek90@gmail.com,
[g] https://orcid.org/0000-0003-1721-2002, bataev@corp.nstu.ru, [h] https://orcid.org/0000-0001-5021-0098, i.ivanov@corp.nstu.ru,
[i] https://orcid.org/0000-0001-5037-245X, sharkeev@ispms.ru

ARTICLE INFO

Article history:
Received: 21 September 2022
Revised: 14 October 2022
Accepted: 03 November 2022
Available online: 15 December 2022

Keywords:
Ti-Nb-Zr alloy
Severe plastic deformation
Ultrafine-grained structure
Mechanical properties
Phase composition

Funding
The work was performed according to the Government Research Assignment for the Institute of Strength Physics and Materials Science of the Siberian Branch of the Russian Academy of Sciences (ISPMS SB RAS), project No. FWRW-2021-0004 (2021-2024). Experimental research was conducted using the equipment of the Common Use Center "Nanotech" at the Institute of Strength, Physics, and Materials Science, SB RAS (ISPMS SB RAS, Tomsk, Russia).

ABSTRACT

Introduction. The interest of modern medical materials science is focused on the development of beta-alloys of ternary systems (*TNZ*) based on titanium, niobium and zirconium with the low Young's modulus, which is comparable with the elastic modulus of the bone. A wide application of the above alloys in medicine is limited by its insufficiently high strength properties, such as yield strength, ultimate strength, fatigue strength, fatigue life, etc. The formation of bulk ultrafine-grained structure in the alloys via deformation processing, including severe plastic deformation, ensures a considerable increase in the mechanical properties of alloys without toxic alloying elements. **The aim of** the work is to analyze the influence of deformation (multipass rolling and *abc*-pressing in combination with rolling) on the microstructure and mechanical properties of the alloy of the Ti-Nb-Zr system. **The research methods**. The Ti-42Nb-7Zr alloy cast blanks were made from pure titanium, niobium, and zirconium iodides by arc melting with a tungsten electrode in the protective argon atmosphere. It is shown that the cast blanks obtained have a high degree of uniformity in the distribution of niobium and zirconium alloying elements. To form an ultrafine-grained (*UFG*) structure, the cast blanks were subjected to deformation according to two schemes: 1) multipass rolling and 2) a combined method of severe plastic deformation, consisting in *abc*-pressing and subsequent multipass groove rolling. **Results and discussion**. As a result of deformation processing by rolling, an ultrafine-grained (*UFG*) structure is formed, which is represented by non-equiaxed β-subgrains with cross-sectional dimensions 0.2…0.8 μm and length 0.2…0.7 μm, dispersion strengthened nanosized ω-phase, as well as subgrains of the α''-phase. Application of combined severe plastic deformation has promoted formation of a more dispersed *UFG* (β+ω)-structure with an average size of structural elements equal to 0.3 μm. The *UFG* structure formed as a result of two-stage *SPD* has provided a high level of mechanical properties: yield strength – 480 MPa, ultimate strength – 1.100 MPa, microhardness – 2.800 MPa, with a low modulus of elasticity equal to 36 GPa.

For citation: Eroshenko A.Yu., Legostaeva E.V., Glukhov I.A., Uvarkin P.V., Tolmachev A.I., Luginin N.A., Bataev V.A., Ivanov I.V., Sharkeev Yu.P. Effect of deformation processing on microstructure and mechanical properties of Ti-42Nb-7Zr alloy. *Obrabotka metallov (tekhnologiya, oborudovanie, instrumenty) = Metal Working and Material Science*, 2022, vol. 24, no. 4, pp. 206–218. DOI: 10.17212/1994-6309-2022-24.4-206-218. (In Russian).

*** Corresponding author**
Eroshenko Anna Yu., Ph.D. (Engineering), Senior Researcher
Institute of Physics of Strength and Materials Science, SB of RAS,
2/4 Akademicheskiy Ave.
634055, Tomsk, Russian Federation
Tel.: 8 (3822) 28-69-11, **e-mail:** eroshenko@ispms.ru

Introduction

The design of metallic materials for medical purposes, combining high mechanical properties and low elastic modulus, as well as mechanical and biological compatibility, is an important challenge today [1]. In this regard, a promising trend in the field of medical materials science is the development of titanium-based alloys doped with bioinert metals that do not have a toxic effect on human body. These are alloys of the following systems: *Ti-Nb*, *Ti-Nb-Ta*, *Ti-Nb-Zr*, *Ti-Nb-Sn*, *Ti-Nb-Ta*, *Ti-Nb-Hf*, *Ti-Nb-Zr-Sn*, *Ti-Nb-Ta-Sn*, *Ti-Nb-Ta-Zr* [1, 2]. The alloying of titanium with stabilizing elements of certain concentrations, such as niobium, zirconium, and tantalum, allows the formation of a β-phase that contributes to a low modulus of elasticity in the alloy. The elastic modulus of such alloys, depending on the elemental composition, can vary in the range of 14–50 GPa, which is comparable with the elastic modulus of bone tissue (10–30 GPa) [2]. The interest in alloys with a low modulus of elasticity is reflected in a number of scientific studies carried out for alloys of ternary systems based on titanium, niobium and zirconium *(TNZ)*: *Ti-13Zr-13Nb*, *Ti-19Nb-14Zr*, *Ti-Nb(18-19)-Zr(5-6)* [3–8]. The advantage of *TNZ* alloys is the absence of toxic effects on the body. However, its wide application in medicine is limited by its low strength properties, such as yield strength, ultimate strength, fatigue strength, etc.

The formation of an ultrafine-grained (*UFG*) structure in β-titanium alloys by the severe plastic deformation (*SPD*) method provides a significant increase in fatigue strength and cyclic durability without alloying with "toxic" elements and increases the strength and yield strength up to the level of coarse-grained (*CG*) medium-strength "α + β" titanium alloys for medical applications. It was shown in [9] that, depending on the modes of thermomechanical treatments, the elastic modulus of the *Ti-13Nb-13Zr* alloy ranges from 79–84 GPa. For *Ti-Nb-Zr* alloys with different concentrations of niobium and zirconium after rolling and heat treatment, the elastic modulus and ultimate strength can vary from 59 to 75 GPa and from 345 to 810 MPa, respectively [9–11].

However, the issues related to achieving the required mechanical properties and the regularities of structure formation during *SPD* require further development due to the large variety of forming structures and phase transformations for multicomponent systems based on titanium with a stabilized β-phase and low modulus of elasticity. All these factors determine the relevance of the research aimed at designing alloys based on titanium, niobium, zirconium and further solving problems associated with increasing the level of mechanical properties and reducing the value of the elastic modulus.

The aim of the work is to reveal the effect of severe plastic deformation on the microstructure and mechanical properties of an alloy of the *Ti-Nb-Zr* system.

Materials and research methodology

The alloy of the *Ti-Nb-Zr* system, *Ti-42Nb-7Zr*, was used as a research material. The experimental *Ti-42Nb-7Zr* alloy ingots were fabricated from pure iodide titanium, niobium, and iodide zirconium by arc melting in a shielding argon atmosphere using a non-consumable tungsten electrode in a *Buhler* furnace [12]. To ensure the homogeneity of the chemical composition, a fivefold remelting was carried out. The ingots were obtained in the form of disks (diameter – 25 mm, height – 8 mm) with a mass of 20 g. According to the X-ray microanalysis data, the ingots had the following composition (wt %): *Ti* – 50.3; *Nb* – 42.3; *Zr*– 7.4. After remelting, the ingots were held at 1,000 °C for 3 hours in an argon atmosphere and subsequently quenched in water. Billets were prepared from the ingots and subjected to heat treatment and *SPD* according to two schemes to obtain the *UFG* state. Figure 1 shows the schemes of thermal and deformation treatments of the alloy ingots.

According to the first scheme, billets in the form of parallelepipeds with the dimensions of 7×8×15 mm^3 were cut from the ingot by an electrospark discharge machine. Then billets were subjected to *SPD*, which consisted of multi-pass flat rolling. Before rolling, the billets were preheated to 200 °C, and the rolling was carried out in the room temperature rolls to a total logarithmic strain of 2.19.

In the second scheme, a combined *SPD* method was used, consisting of *abc*-pressing and subsequent multi-pass rolling in grooved and then in flat rolls. A billet with the dimensions of 13×15×18 mm^3 was

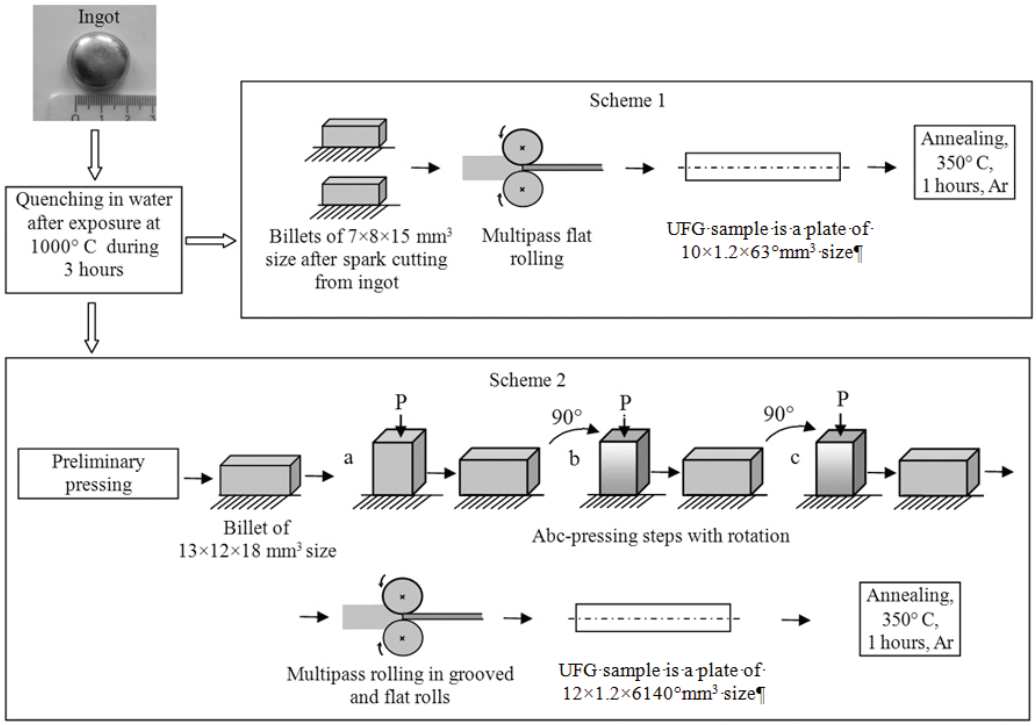

Fig. 1. Scheme of heat and deformation treatments of *Ti-42Nb-7Zr* alloy

obtained from the ingot as a result of pre-pressing. *Abc*-pressing of the billet was carried out with a step decrease in temperature from 500 to 400 °C. In this case, a single upsetting of the billet at each temperature was performed. Rolling of preheated billets to 200 °C was carried out, as in the case of the first scheme, at the room temperature of the rolls. In this case, the total logarithmic degree of deformation was 2.94. After the application of the first and second schemes, plates with dimensions of 10×1.5×140 mm^3 were obtained.

The prepared samples were annealed at 350 °C for one hour in an argon atmosphere and then cooled with the furnace to remove residual internal stresses and to increase plasticity. For a comparative study of *UFG* states with a *CG* structure, we used recrystallization annealing of a part of the samples at 800 °C for one hour after the second scheme of deformation.

The microstructure and phase composition of the samples were studied using optical microscopy (*Carl Zeiss Axio Observer* microscope), transmission electron and scanning electron microscopy (*JEOL JEM* 2100 and *LEO EVO* 50 microscopes), as well as X-ray diffractometry (*DRON-7* diffractometer). The X-ray diffraction patterns were obtained in *CoK*α radiation. The average size of structural elements (grains, subgrains, fragments) was calculated using the secant line method [14]. The microhardness was measured using the *Duramin* 5 microhardness tester. The mechanical tensile tests were performed on the *Instron* 5582 testing machine. During mechanical testing, five samples were used for each state. The elastic modulus was determined using the *DUH-211S* Nano Hardness Tester by pressing the indenter into the surface of the sample with simultaneous plotting of the "stress–strain" kinetic diagram. The microstructural and X-ray diffraction studies, as well as measurements of microhardness and mechanical tests of the samples were carried out for the *CG* state and for the *UFG* states obtained after rolling and after combined deformation impact (*abc*-pressing and rolling).

Results and discussion

Fig. 2, *a*, *b* shows the microstructure of the *Ti-42Nb-7Zr* ingots after remelting. The microstructure is heterogeneous across the cross-section of the ingot in the cast state. Three zones are readily observed. The first zone consists of equiaxed grains. The second and third zones have a dendritic structure, where the second zone is region with a cellular structure, and the third zone is a region of elongated columnar dendrites.

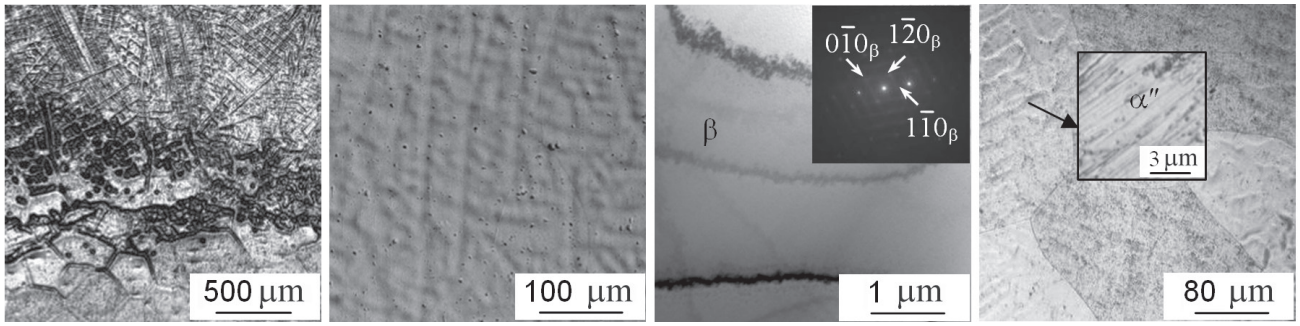

a *b* *c* *d*

Fig. 2. Optical (*a, d*), *SEM* (*b*) and *TEM* images with corresponding microdiffraction patterns (*c*) of *Ti-42Nb-7Z* alloy microstructure:
cast (*a, b, c)*; quenched (*d*) states

The presence of columnar dendrites indicates liquation in the β-solid solution during remelting [15]. The X-ray microanalysis study showed that the ingots after remelting had a high degree of uniformity of the distribution of alloying elements (niobium and zirconium) by volume. The concentration of niobium over the cross-section of the ingot was in the range of 41.2–43.1 wt. %, while the zirconium concentration was 6.8–7.3 wt. %.

A characteristic feature of the ingot microstructure was the developed dendritic structure in its upper part and a coarse-grained structure with grains dimensions of 200-500 μm based on a solid solution of titanium and/or niobium in its lower part. According to the *TEM* data, the main phase in the alloy is the β-phase based on a solid solution (Fig. 2, *c*). Before deformation impact, the alloy was subjected to quenching, which consisted in holding at a temperature of 1,000 °C for 3 hours, followed by cooling in water at room temperature. The optical image of the microstructure of the alloy after quenching is shown in Fig. 2, *d*. The microstructure is homogeneous over the cross-section of the ingot. In the structure, equiaxed grains of the β-phase and plates of the martensitic α″-phase are observed, which are characteristic of the structure after quenching. Formation of the martensite α″-phase is characteristic of titanium-based β-alloys due to the high niobium content. Thus, for the *Ti–Nb* system, the formation of a martensitic α″-phase is observed in hardened alloys containing niobium in the concentration range from 30 to 40 wt % [15, 16]. The average grain size of the β-phase was 100 μm.

The microstructure of the hardened alloy after multi-pass rolling is presented in Fig. 3. Rolling leads to the formation of a strip character of the microstructure. In bright-field images, the "stripe" fragments with cross-sectional dimensions of 0.2-0.8 μm and a length of 0.2-0.7 μm are observed. This corresponds to the *UFG* state according to the classification given in [17]. In the stripe fragments, the formation of a dislocation substructure is observed. The stripe fragments consist of a β-phase based on a solid solution of titanium and niobium (Fig. 3, *a*, *b*) On the bright-field images in the local areas, there are precipitates of the second α″-phase in the form of 10 nm wide plates, which are localized inside the subgrains of the matrix β-phase (Fig. 3, *c*). The microdiffraction pattern (Fig. 3, *c*) is represented by point reflexes. Moreover, Fig. 3, *b* shows the scheme of microdiffraction pattern identification, in which reflexes corresponding to the nanodispersed ω-phase particles were distinguished in the grid of the β-phase reflexes. On the dark-field image obtained in reflexes from the β-and ω-phases, the nanoparticles of the ω-phase with a size of 10 nm are visible inside the β-phase bands (Fig. 3, *d*).

Figure 4 *a*, *b* shows the *TEM* images of the microstructure of the *Ti-42Nb-7Zr* alloy subjected to *abc*-pressing followed by rolling (the second scheme). The microstructure has a less pronounced "band" character (Fig. 4, *a*). As a result of combined *SPD*, non-equiaxed subgrains of the β-phase are formed, in which there are dispersed nanoparticles of the ω-phase (Fig. 4, *b*). In the β-phase subgrains the developed dislocation substructure with an increased density of dislocations is observed. The reflexes in the microdiffraction pattern are located in circles, which indicates the significant refinement of the structure after deformation, as well as the presence of high-angle grain boundaries. Subgrains of the β-phase have sizes in the range of

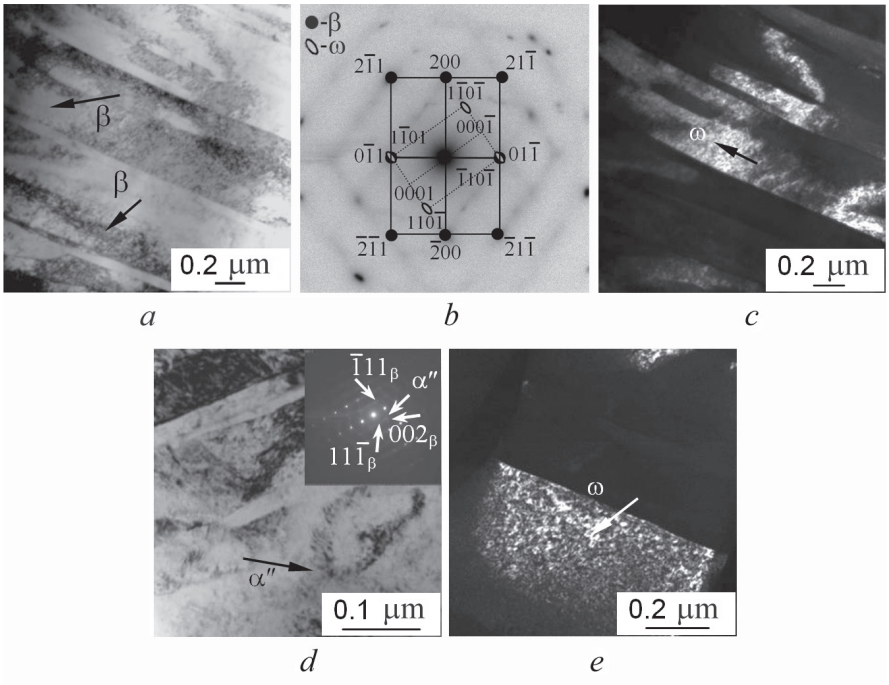

Fig. 3. TEM images of the quenched *Ti-42Nb-7Zr* alloy microstructure after rolling: bright field with corresponding microdiffraction patterns (*a, d*) and dark field (*b, c*) images; microdiffraction pattern identification scheme (*b*)

0.1–0.6 μm. The average size of the structural elements is 0.3 μm. Inside the fragments of the main β-phase, nanoparticles of the ω-phase are observed (Fig. 4, *d*). It should be noted that during the combined *SPD* process, the plates of the martensitic α″-phase could not be detected. This is apparently due to the fact that during pressing in the temperature range of 500–400 °C, the martensitic α″-phase was transformed into the β-phase according to the mechanism α″→α→β [18–20].

It is necessary to note that the use of *abc*-pressing with rolling of alloy billets leads to the formation of a more dispersed *UFG* microstructure compared to rolling without the pressing stage.

The microstructure of the *Ti-42Nb-7Zr* alloy in the *CG* recrystallized state, obtained by annealing the sample in the *UFG* state at a temperature 800 °C, consists of equiaxed polyhedral grains of the matrix β-phase (Fig. 4, *c*). The average β-grain size is 20 μm. Inside the matrix β-grains, there are ω-phase nanoparticles with an average size of 10 nm (Fig. 4, *d*).

Figure 5 shows the X-ray diffraction patterns for the *Ti-42Nb-7Zr* alloy in various states. In the cast state, the phase composition is represented by a β-phase based on a solid solution of titanium and niobium (Fig. 5, *a*). In the quenched state (Fig. 5, *b*) and after rolling (Fig. 5, *c*), in addition to the main β-phase, there

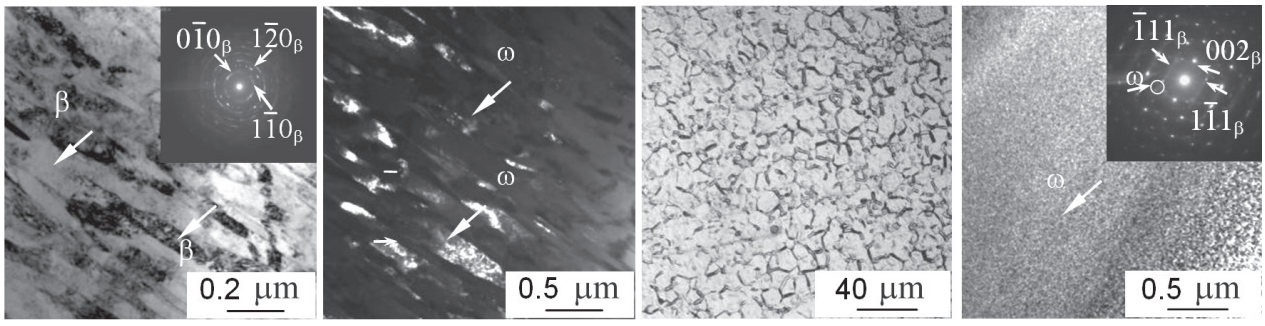

Fig. 4. TEM and optical images of *Ti-42Nb-7Zr UFG* alloy microstructure after *abc*-pressing with rolling (*a, b*) and in the recrystallized state (*c, d*):

bright field with the corresponding microdiffraction patterns (*a, d*); dark field (*b*); optical (*c*) images

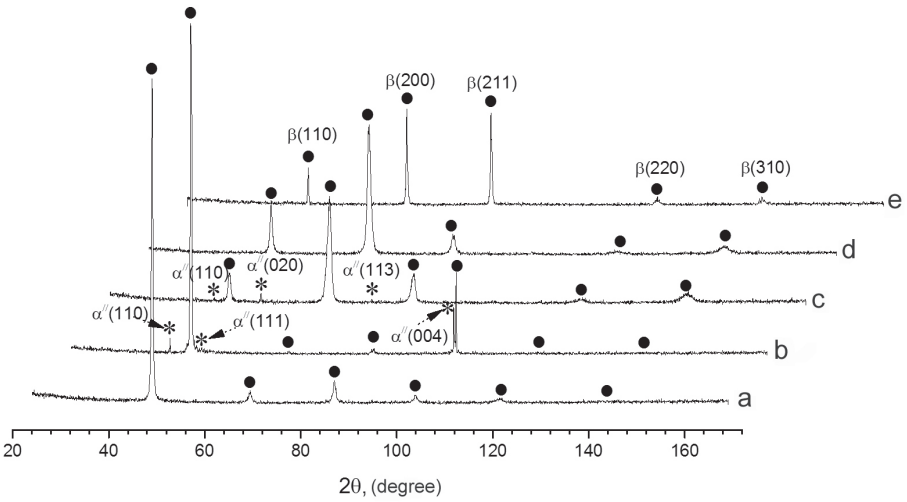

Fig. 5. X-ray diffraction pattern of *Ti-42Nb-7Zr* alloy in different states: cast (*a*); quenched (*b*); *UFG*, rolling (*c*); *UFG*, *abc*-pressing with rolling (*d*); *CG* (*e*)

are low intensity reflexes from the second phase, α″-martensite, which was formed during rapid cooling in the areas depleted of alloying elements [15].

At the same time, in the state after the combined *SPD* method, the α″-phase reflexes are not detected on the X-ray diffraction patterns, there are reflexes belonging only to the β-phase (Fig. 5, *d*). In this case, a noticeable increase in the width of X-ray lines is observed after the deformation of the alloy, which indicates the formation of the developed dislocation substructure.

In the recrystallized *CG* state, the reflexes from the β-phase are observed in the X-ray diffractogram (Fig. 5, *e*). It should be pointed out that the ω-phase could not be identified by the X-ray diffraction analysis, probably due to its small volume fraction.

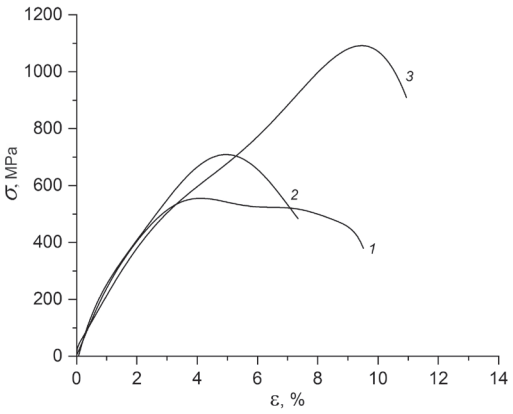

Fig 6. Engineering curves for *Ti-42Nb-7Zr* alloy samples in different states: *1 – CG*; *2 – UFG* (rolling); *3 – UFG* (*abc*-pressing with rolling)

Thus, according to the given results, as a result of rolling of the alloy samples, a stripe *UFG* microstructure is formed. It is represented by β-subgrains, dispersion strengthened by the nano-sized ω-phase, and a small amount of α″-martensite. The use of multi-pass rolling after *abc*-pressing leads to the formation of a more dispersed *UFG* structure, represented by β-subgrains, dispersion strengthened by ω-phase nanoparticles.

Figure 6 shows the engineering curves of the *Ti-42Nb-7Zr* alloy samples during static tensile tests for different states. It should be noted that, due to the small size of the samples in the initial cast state and in the state after quenching, it was not possible to evaluate its tensile properties. Therefore, the mechanical properties of the *UFG* alloy samples were compared with those in the *CG* (recrystallized) state.

The tensile tests have shown that after multi-pass rolling of the hardened state samples the following mechanical properties are achieved: offset yield strength ($\sigma_{0.2}$) is 390 MPa, the ultimate strength (σ_u) is 710 MPa and the fracture strain (ε_f) is 5.7 %. It can be seen that for the *UFG* alloy formed as a result of multi-pass rolling, the ultimate strength is 1.3 times higher compared to the *CG* state. It is worth noting that in this case the value of the offset yield strength for the *UFG* alloy does not differ from that of the *CG* alloy, which is associated with its dispersion strengthening by the ω-phase particles. After the combined *SPD* the alloy samples have the maximum mechanical characteristics, namely: the offset yield strength ($\sigma_{0.2}$) is 480 MPa and the ultimate strength (σ_u) is 1,100 MPa at the fracture strain (ε_f) equaled to 4.6 %. Grain refinement as a result of the two-stage *SPD* leads to an increase in the yield strength by more

than 1.3 times and in the ultimate strength by 2 times in comparison with the *CG* state. Significant strengthening of the samples after the combined *SPD* in comparison with the multi-pass rolling is associated with additional refinement of structural elements.

The mechanical properties and the structural-phase characteristics of the *Ti-42Nb-7Zr* alloy in different states are shown in Table.

Mechanical and structural phase characteristics of the alloy in different states

State	Average size of main β-phase elements, μm	Phase composition	$\sigma_{0.2}$, MPa	σ_u, MPa	ε_f, %	H_μ, MPa
Cast	– dendrites up to 500 μm long; – equiaxed grains 350 ± 100	β	–	–	–	1,900 ± 200
Quenched	equiaxed grains 100 ± 30	β + α″	–	–	–	1,540 ± 100
CG	equiaxed grains 20 ± 5	(β + ω)	350 ± 20	550 ± 30	8.7 ± 0,2	1,700 ± 100
UFG (rolling)	bands: – length (0.2–0.8) – width (0.2–0.7)	(β + ω) + α″	390 ± 30	710 ± 50	5.7 ± 0,3	2,570 ± 100
UFG (*abc*-pressing+ +rolling)	non-equiaxed grains 0.3 ± 0.2	(β + ω)	480 ± 30	1,100 ± 50	4.6 ± 0,3	2,800 ± 100

For comparison, Table shows the microhardness value for the *CG* state of the alloy. The formation of the *UFG* structure in the alloy as a result of multi-pass rolling and the combined *SPD* method leads to an increase in the microhardness level to 2,570 and 2,800 MPa, which is 1.6 and 1.8 times higher, respectively, compared to the *CG* state (1,700 MPa).

The value of the elastic modulus of the *UFG* alloy formed by the combined *SPD* method is 36 GPa, and for the *CG* state it is 42 GPa, which is significantly lower than for medium-strength titanium alloys, *Ti-6Al-4V ELI*, *Ti-6Al-4V*, and the pure titanium (100–110 GPa), that are widely used in medicine [21].

Thus, the *UFG* (β + ω) structure obtained by the combined *SPD* method with an average size of structural elements equaled to 0.3 μm, makes it possible to achieve a higher level of mechanical properties in the *Ti-42Nb-7Zr* alloy as compared to the structure after rolling. A significant increase in the offset yield strength and ultimate strength, as well as microhardness after deformation in the *UFG* alloy is associated with substructural and dispersion strengthening.

Conclusions

The multi-pass cold rolling of the *Ti-42Nb-7Zr* alloy in the quenched state leads to the formation of an *UFG* structure that has a stripe character, in which the main phase is the β-phase dispersion strengthened by *ω*-particles, and there is also a small amount of precipitates of the α″-martensite phase.

The combined *SPD* method of the *Ti-42Nb-7Zr* alloy promotes more efficient grain refinement and the formation of a more dispersed *UFG* structure with an average size of structural elements of 0.3 μm, represented by β-subgrains that are dispersion strengthened by ω-phase nanoparticles. The martensitic α″-phase transforms into the β-phase by the α″→α→β mechanism and is not observed after the combined *SPD*.

The formed *UFG* state with (β + ω)-structure in the *Ti-42Nb-7Zr* alloy as a result of the combined *SPD* method provides a significant increase in mechanical properties: offset yield strength is 480 MPa, ultimate strength is 1,100 MPa, microhardness is 2,800 MPa at the fracture strain of 4.6 %, which is associated with substructural and dispersion strengthening.

References

1. Niinomi M. Recent metallic materials for biomedical applications. *Metallurgical and Materials Transactions A*, 2002, vol. 33, pp. 477–486. DOI: 10.1007/s11661-002-0109-2.

2. Liang S.X., Feng X.J., Yin L.X., Liu X.Y., Ma M.Z., Liu R.P. Development of a new β Ti alloy with low modulus and favorable plasticity for implant material. *Materials Science and Engineering: C*, 2016, vol. 61, pp. 338–343. DOI: 10.1016/j.msec.2015.12.076.

3. Nune K.C., Misra R.D., Li S.J., Hao Y.L., Yang R. Osteoblast cellular activity on low elastic modulus Ti-24Nb-4Zr-8Sn alloy. *Dental Materials*, 2017, vol. 33, pp. 152–165. DOI: 10.1016/j.dental.2016.11.005.

4. Cheng J., Li J., Yu S., Du Z., Zhang X., Zhang W., Gai J., Wang H., Song H., Yu Z. Cold rolling deformation characteristic of a biomedical beta type ti–25nb–3zr–2sn–3mo alloy plate and its influence on α precipitated phases and room temperature mechanical properties during aging treatment. *Frontiers in Bioengineering and Biotechnology*, 2020, vol. 8, p. 598529. DOI: 10.3389/fbioe.2020.598529.

5. Li T., Kent D., Sha G., Dargusch M.S., Cairney J.M. Precipitation of the α-phase in an ultrafine grained beta-titanium alloy processed by severe plastic deformation. *Materials Science and Engineering: A*, 2014, vol. 605, pp. 144–150. DOI: 10.1016/j.msea.2014.03.044.

6. Prokoshkin S., Bralovski V., Dubinskiy S., Zhukova Y., Sheremetyev V., Konopatsky A., Inaekyan K. Manufacturing, structure control, and functional testing of Ti–Nb-based SMA for medical application. *Shape Memory and Superelasticity*, 2016, vol. 3, pp. 130–144. DOI: 10.1007/s40830-016-0059-y.

7. Sun F., Hao Y.L, Nowak S., Gloriant T., Laheurte P., Prima F. A thermo-mechanical treatment to improve the superelastic performances of biomedical Ti–26Nb and Ti–20Nb–6Zr (at.%) alloys. *Journal of the Mechanical Behavior of Biomedical Materials*, 2011, vol. 4, pp. 1864–1872. DOI: 10.1016/j.jmbbm.2011.06.003.

8. Dimic I., Cvijovic-Alagic I., Volker B., Hohenwarter A., Pipan R., Veljovic D., Rakin M., Bugarski B. Microstructure and metallic ion release of pure titanium and Ti–13Nb–13Zr alloy processed by high pressure torsion. *Materials and Design*, 2016, vol. 91 (5), pp. 340–347. DOI: 10.1016/j.matdes.2015.11.088.

9. Chneider S.G., Nunes C.A., Rogero S.O., Higa O.Z., Bressiani J.C. Mechanical properties and cytotoxic evaluation of the Ti-3Nb-13Zr alloy. *Biomecánica*, 2000, vol. 8 (1), pp. 84–87. DOI: 10.5821/sibb.v8i1.1653.

10. Ozan S., Lin J., Li Yu., Munir K., Jiang H., Wen C. Deformation mechanism and mechanical properties of a thermomechanically processed β Ti–28Nb–35.4Zr alloy. *Journal of the Mechanical Behavior of Biomedical Materials*, 2018, vol. 78, pp. 224–234. DOI: 10.1016/j.jmbbm.2017.11.025.

11. Ozan S., Lin J., Zhang Y., Li Yu., Wen C. Cold rolling deformation and annealing behavior of a β-type Ti–34Nb–25Zr titanium alloy for biomedical applications. *Journal of Materials Research and Technology*, 2020, vol. 9 (2), pp. 2308–2318. DOI: 10.1016/j.jmrt.2019.12.062.

12. Ivanov I.V., Thoemmes A., Skiba V.Yu., Ruktuev A.A., Bataev I.A. Effect of electron beam power density on the structure of titanium under non-vacuum electron-beam treatment. *Metal Science and Heat Treatment*, 2019, vol. 60, pp. 625–632. DOI: 10.1007/s11041-019-00329-x.

13. Sharkeev Yu.P., Eroshenko A.Yu., Glukhov I.A., Tolmachev A.I., Zhu Q. Microstructure and mechanical properties of Ti40Nb alloy after severe plastic deformation. *AIP Conference Proceedings*, 2014, vol. 1623, pp. 567–570. DOI: 10.1063/1.4899008.

14. ASTM E1382-97. *Standard test methods for determining average grain size using semiautomatic and automatic image analysis*. West Conshohocken, PA, ASTM International, 2016. 24 p.

15. Collings E.W. *Physical metallurgy of titanium alloys*. Metals Park, OH, American Society for Metals, 1984. 261 p. ISBN 9780871701817.

16. Inamura T., Kim J.I., Kim H.Y., Hosoda H., Wakashima K., Miyazaki S. Composition dependent crystallography of α″-martensite in Ti–Nb-based β-titanium alloy. *Philosophical Magazine*, 2007, vol. 87, iss. 23, pp. 3325–3350. DOI: 10.1080/14786430601003874.

17. Glezer A.M., Kozlov E.V., Koneva N.A., Popova N.A., Kurzina I.A. *Plastic deformation of nanostructured materials*. Boca Raton, CRC Press, 2017. 334 p. ISBN 9780367573201.

18. Bonisch M., Panigrahi A., Calin M., Waitz T., Zehetbauer M., Skrotzki W., Eckert J. Thermal stability and latent heat of Nb–rich martensitic Ti-Nb alloys. *Journal of Alloys and Compounds*, 2017, vol. 697, pp. 300–309. DOI: 10.1016/j.jallcom.2016.12.108.

19. Banerjee S., Mukhopadhyay P. *Phase transformations*. Amsterdam, Elsevier, 2007. 813 p. ISBN 9780080548791.

20. Ozan S., Lin J., Weng W., Zhang Y., Li Yu., Wen C. Effect of thermomechanical treatment on the mechanical and microstructural evolution of a β-type Ti-40.7Zr–24.8Nb alloy. *Bioactive Materials*, 2019, vol. 4, pp. 303–311. DOI: 10.1016/j.bioactmat.2019.10.007.

21. Niinomi M., Liu Y., Nakai M., Lui H., Li H. Biomedical titanium alloys with Young's moduli close to that of cortical bone. *Regenerative Biomaterials*, 2016, vol. 3, pp. 173–185. DOI: 10.1093/rb/rbw016.

Conflicts of Interest

The authors declare no conflict of interest.